ION BEAM FACILITY
ANNUAL REPORT 2022

DIFFER

DIFFER

SCIENCE FOR **FUTURE ENERGY**

ION BEAM FACILITY
ANNUAL REPORT 2022

Ion Beam Facility Annual Report 2022

This report summarizes the activities at the DIFFER Ion Beam Facility (IBF) in 2022. The accelerator was used for 1152 hours within 137 days to conduct research (100% ion beam analysis) and 65 days were spent on mainly repairs but also maintenance and implementation of lab improvements such as the magnetic compensation system or CODAC. The report gives a short summary of the academic research and performed repairs/maintenance.

Facility Manager	Dr. Hans van Eck
Project Leader	Dr. Beata Tyburska-Pueschel
Accelerator operator	Wim Melissen
Radiation safety	Santi Alonso van den Westen

https://www.differ.nl/research/fusion-facilities-and-instrumentation/ion-beam-facility

De Zaale 20
5612 AJ Eindhoven, The Netherlands

IBF in numbers

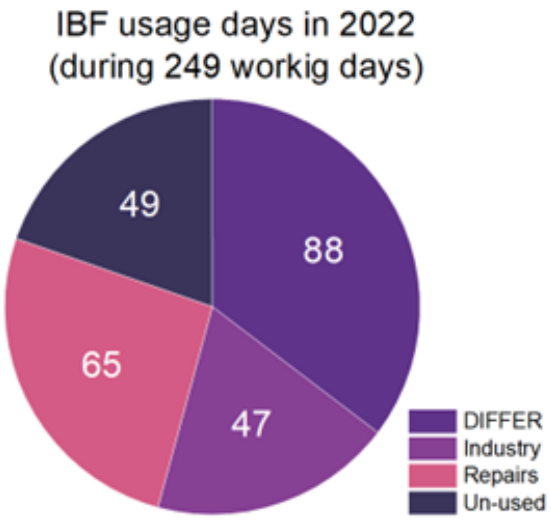

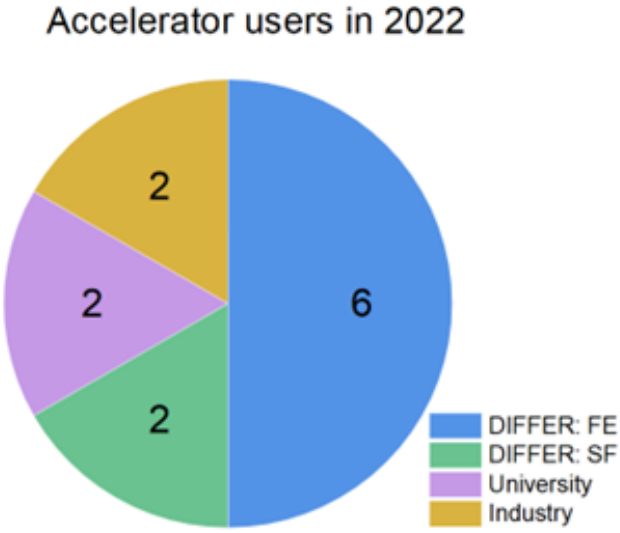

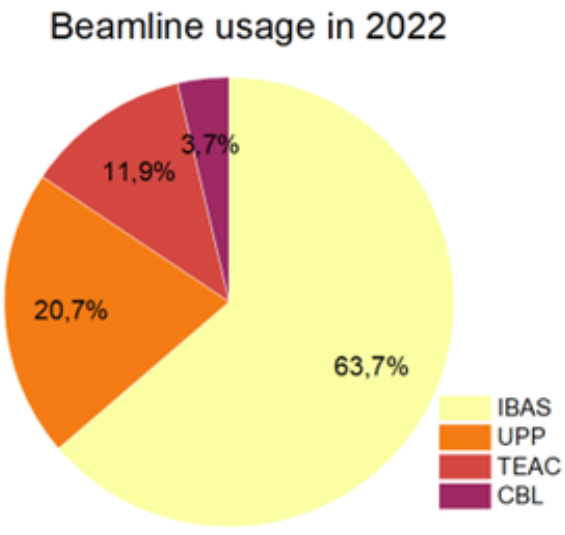

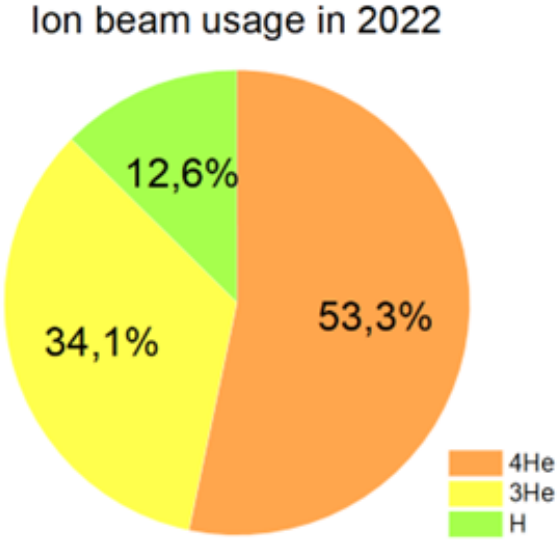

Aliovalent calcium doping of yttrium oxyhydride thin films and implications for photochromism

D. Chaykina (TU Delft) and B. Tyburska-Pueschel (DIFFER)

Rare-earth metal oxyhydride thin films exhibit a photochromic effect; when exposed to UV light, these materials change from transparent to opaque, but return to their transparency state when the light is removed. The mechanism behind this effect is not known and it is difficult to find a direct technique which will reveal the answer. It is suspected that the anions (H^- and O^{2-}) are important for the effect since their ratio in the composition of the thin film greatly impacts the speed and extent of color change. Here, by aliovalent doping of yttrium oxyhydride with calcium, we create anion vacancies in order to assess the effect of this on the anion composition and the photochromic properties.

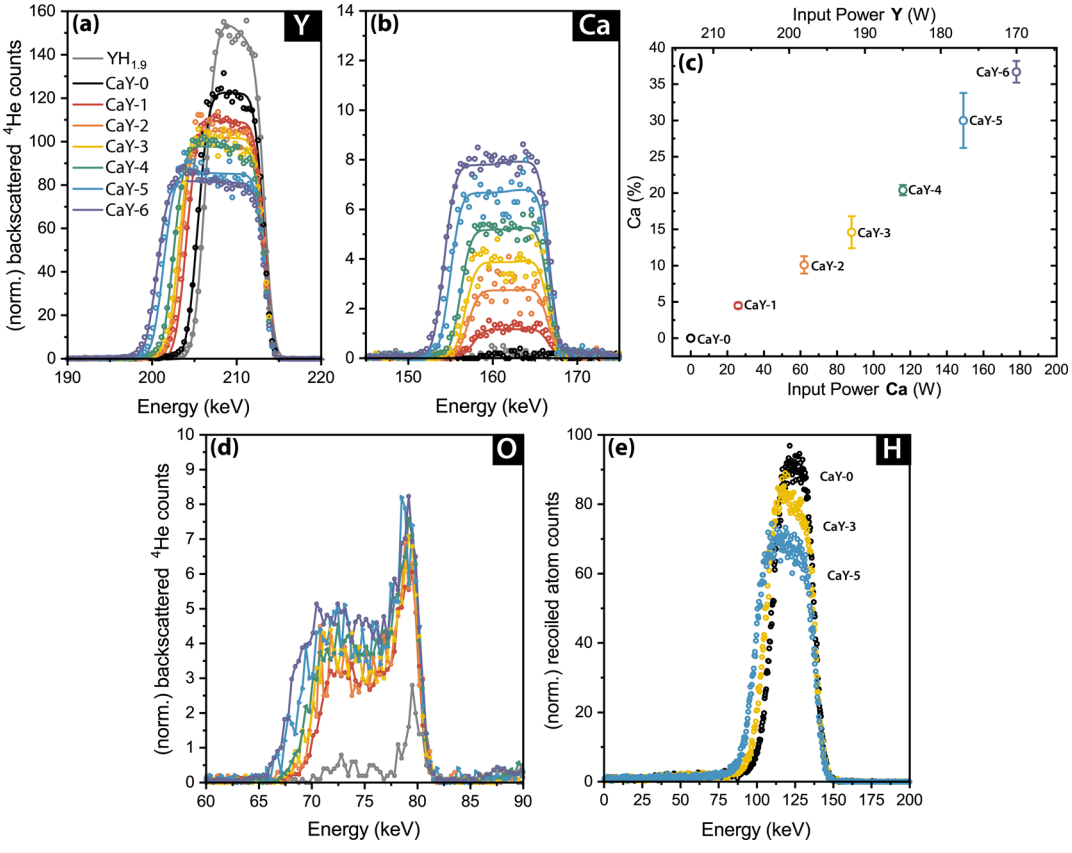

Figure 1 RBS data for (a) yttrium, (b) calcium, and (d) oxygen, along with the (c) calculated Ca/Y content for each sample plotted against the sputtering conditions. (e) The hydrogen content measured by ERD for several films

By RBS, we confirmed that we can change the ratio of Ca to Y by reactive magnetron co-sputtering of Ca- and Y-metal targets (figure 1, a-c). As well, since the increase of Ca should introduce anion vacancies into the structure, the anions (O^{2-}, H^-) were qualitatively assessed by a combination of RBS and ERD (figure 1, d-e). As the amount of Ca increased, the hydride-content decreased significantly, while the oxide-content increased slightly, suggesting that the anion vacancies created are primarily hydride vacancies.

These results are then used to explain the change in photochromic properties of these materials as the Ca-doping level is increased (figure 2). Based on the differences in the relative photochromic contrast (amount of color change after 1 h of illumination) and the bleaching speed (time to return to the transparent state after illumination), we were able to determine that the amount of anion vacancies in the sample is a key ingredient to photochromism.

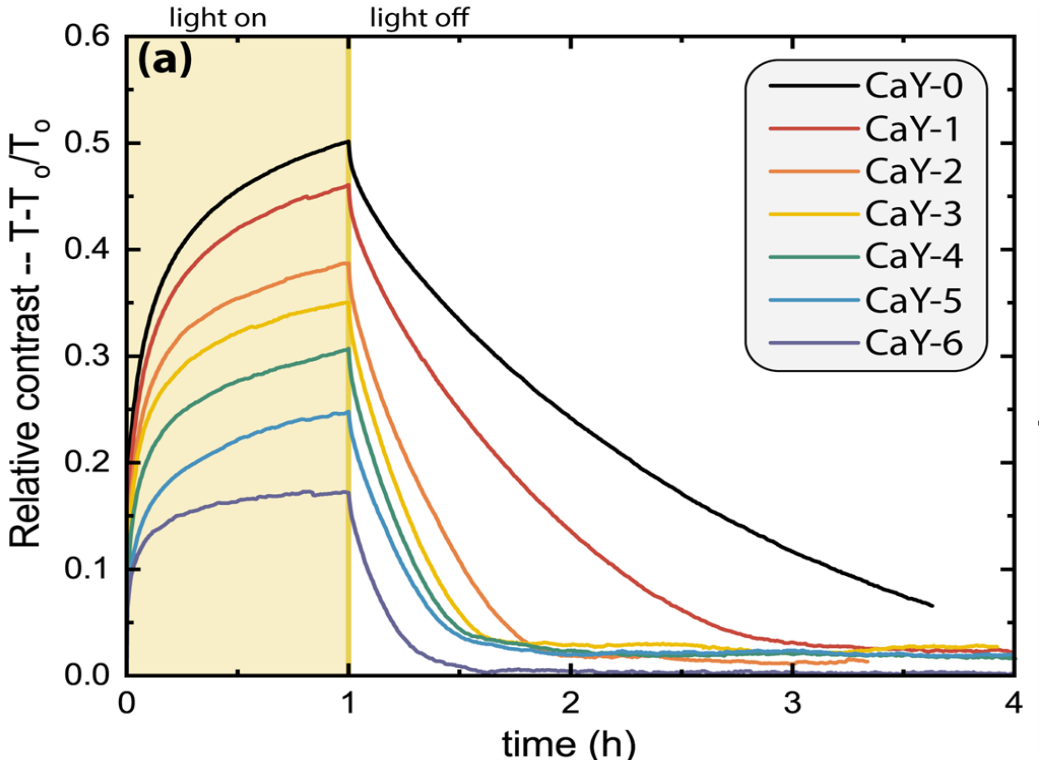

Figure 2 (a) Change in relative photochromic contrast for samples with increasing Ca-content (CaY-0 = 0% Ca CaY-6 = 35% Ca). As the Ca-content increases, the H-content decreases, and this causes a lower relative contrast. On the other hand, the speed with which the sample returns to its transparent state becomes faster with increasing Ca-content due to the increasing number of anion vacancies

Influence of ELMs on deuterium retention and outgassing in tungsten

R.O. Houben, B. Tyburska-Pueschel, and T.W. Morgan (DIFFER)

The tritium inventory in the vacuum vessel is a critical issue for successful operation of fusion reactors. A part of this tritium is retained in the divertor tiles, which will be fully made of tungsten in ITER. The retained tritium makes them radioactive and brittle while influencing the fuel balance in the reactor. The influence of ELMs on the uptake of deuterium in tungsten is unclear. It was expected that transients would de-gas the surface by heating, but previous experimental work shows an increase in retention by transient laser loading, due to diffusion in the tungsten bulk. In this project the effect of pulsed plasma and laser loading under different steady state plasma loadings on deuterium retention in tungsten is studied using nuclear reaction analysis (NRA) and thermal desorption spectroscopy (TDS).

Using NRA, a deuterium depth profile for the first 3 micrometers in tungsten can be measured. RBS measurements give information of surface effects, such as copper or molybdenum deposition, which come from the Magnum-PSI plasma source or clamping ring. By combining NRA and RBS, conclusions can be drawn how and where the deuterium is retained. In the figure below deuterium retention in samples exposed in Magnum-PSI can be seen. One sample is exposed to pulsed plasma and one sample to laser loading, resulting in a same ΔT for 1 ms of 300 K. The red line shows high amount of retained deuterium on the surface. This is due to copper deposition, which is measured with RBS. A factor 10 difference between the concentration of diffused deuterium can be seen on the right hand side of the figure.

Using TDS, the total retained deuterium is measured in the samples to obtain a complete image of the retention. NRA measurements are performed in-situ in upgraded pilot-PSI (UPP), which is directly connected to the IBF and in the ion beam analysis station (IBAS) for samples exposed in Magnum-PSI.

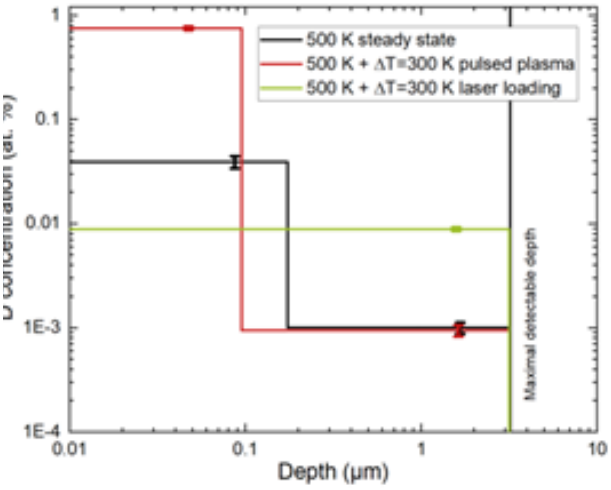

Figure 3 Plot of the depth distribution of retained deuterium for three different samples measured with NRA

Erosion and re-deposition of tungsten under ITER-like plasma conditions

M.J.H. Cornelissen, , B. Tyburska-Pueschel, and T.W. Morgan (DIFFER)

The tungsten divertor of ITER must withstand extreme heat and particle loads. To shield the divertor, ITER is planning to utilize impurity seeding to cool down the plasma by radiation, significantly reducing the heat flux. However, impurities also pose a threat as they are the main contributor to the erosion of the divertor due to their low sputtering threshold energy. In addition, entrainment can occur, which is the acceleration of impurities towards the plasma flow velocity by drag forces, effectively increasing the impurity impact energy. For current tokamaks, the divertor plasma is not dense enough for entrainment to occur, but the high density of ITER's divertor plasma allows for sufficient drag.

While entrainment results in increased sputtering yields, entrainment may also have the benefit of dragging sputtered tungsten back to the surface, effectively decreasing the net erosion rate. To distinguish re-deposition by entrainment from prompt re-deposition, one can investigate the re-deposition location: when re-deposition by entrainment is dominant, an asymmetric re-deposition profile would be expected with more re-deposition downstream of the plasma beam.

In this work, a tungsten target has been exposed to a pure argon plasma in Magnum-PSI (T_e=1.16 eV, n_e=4.7 · 10^{20} m^{-3}) under an angle of 45°. Molybdenum witness plates were positioned around the tungsten target to measure the re-deposition profile (see figure 4). The tungsten target was biased to V=–85 V to allow for considerable sputtering, whereas the witness plates were kept at floating potential. Rutherford backscattering spectroscopy (RBS) was performed with a 2.4 MeV 4He^+ beam to measure the tungsten content on the witness plates. On each of the four witness plates an axial scan has been made of which the results are shown in figure 5. Whereas the deposition profile of tungsten for the left and right witness plates are close to identical, the top witness plate obtained considerably more tungsten than the bottom witness plate. The asymmetry between the top and bottom witness plates is a clear indication of the entrainment of sputtered tungsten back to the surface by the plasma beam: the plasma beam drags the impurities downstream towards the top witness plate.

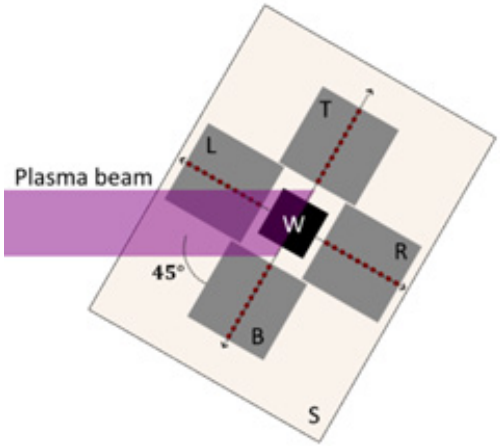

Figure 4 The biased tungsten target (W) is surrounded by four molybdenum witness plates (T, R, B, L), all kept at floating potential by the insulating target holder (S). The red dots indicate the RBS measurement locations. The plasma beam hits the tungsten target under 45°

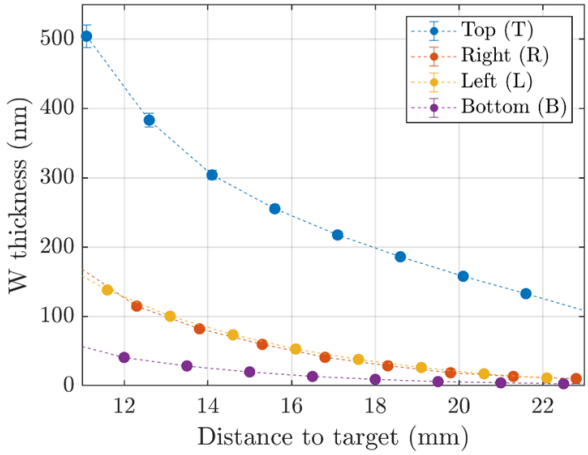

Figure 5 The thickness of the tungsten layer on the four molybdenum witness plates all show an exponential decrease for increasing distances from the target. Whereas the right and left deposition profiles are close to identical, the top and bottom profiles show a clear asymmetry

Depth Profiling of Plasma Irradiated Nickel Nanostructures

Ameya Ranade, B. Tyburska-Pueschel, and Michail Tsampas (DIFFER)

Electrochemical water splitting (via water electrolyzers of photoelectrochemical devices) is considered as a promising source for producing green hydrogen. In the development of water electrolyzers, nickel-based electrocatalysts have garnered special attention because of their favorable characteristics such as high elemental-abundance, high corrosion-resistance, and promising activity towards water splitting reactions. As catalysis is a surface phenomenon, increasing the number of active sites is a commonly employed method to increase the electrochemical performance. Hence, nickel nanostructures were formed by exposing the samples to helium plasma in the Upgraded Pilot PSI (UPP). The growth of in-situ nanostructures have shown to enhance the electrochemical performance by ≈4x along with increased stability than the pristine surfaces.

The as-synthesized nanostructures are typically characterized by various spectroscopic techniques to identify their structural and surface bonding characteristics. However, the changes happening under the first few monolayers are not clearly observed by the commonly used spectral techniques. Focused Ion Beam (FIB) is a method which can determine the approximate thickness of the samples. However, majority of such techniques are either destructive and/or identifying the depth-profile of the elements remains a challenge. Hence, IBA was used to determine the elemental composition of the nickel nanostructures before and after performing electrochemical reactions.

As shown in Figure 6 *a)*, the as-synthesized nickel nanostructures are readily oxidized on exposure to air. However, molybdenum impurities from the UPP (either from the plasma source or clamping ring) were also observed on the surface. After performing the electrochemical reactions, majority of the molybdenum is leached out. Additionally, the ratio between the nickel and oxygen content indicates that nickel is present in higher oxidation states on the surface. Along the depth, this ratio is progressively reduced before becoming completely metallic. Moving forward, these methods can better assist in determining the activity-stability relationships of emerging electrocatalysts.

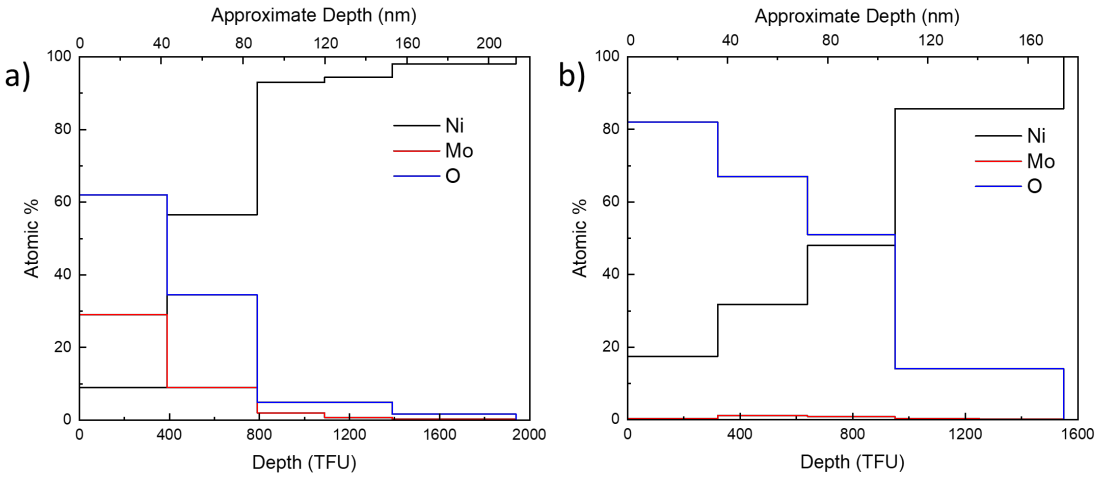

Figure 6 Depth profile of samples a) before electrochemical reaction; b) after electrochemical reaction

Reducing tin droplet ejection from capillary porous structures under hydrogen plasma exposure in Magnum-PSI

Jos Scholte and Tom Morgan (DIFFER)

Liquid metal divertors are a promising alternative to the solid tungsten monoblocks. One of liquid metals currently considered is tin. A disadvantage of Sn is that it is prone to droplet ejection when exposed to a hydrogen plasma (W. Ou *et al.*, Nucl. Fusion 61 (2021) 066030). Hypothesized is that the pore size of the capillary porous structure (CPS) that confines the Sn is an important factor to reduce this phenomena. Therefore different stainless steel targets with a pore size ranging between 0.5 and 100 µm have been exposed to Magnum-PSI. RBS has been used to post-mortem determine the amount of Sn on nearby witness plates. Furthermore, three different tungsten CPSs have been tested to determine, which one reduces Sn droplets the most.

Table 1 Sn erosion from tungsten surfaces as observed by the OES during plasma exposure and RBS on the WPs. An abundance of emission lines were observed during the exposure of the W felts, most of which were saturated, hence the nan. This is most likely due to contamination of the target. The Phantom images in TRACK did show false positives; however, the exact number is unknown. Therefore, the number given in this table serves as an upper boundary

W target	Pore size	Δm_{Sn} [µg]	$\lambda_{SnI}/\lambda_{\zeta}$	T_{max} [°C]	Sn droplet on Phantom camera [s^{-1}]
Felt	~1	33.8±4.8	Nan	1319±3	<1
Sintered	0.65±0.32	13.7±1.0	0.98±0.20	1011±2.7	<375
3D-printed	100±10	331.2±21.9	1.92±0.21	1105±1	<20

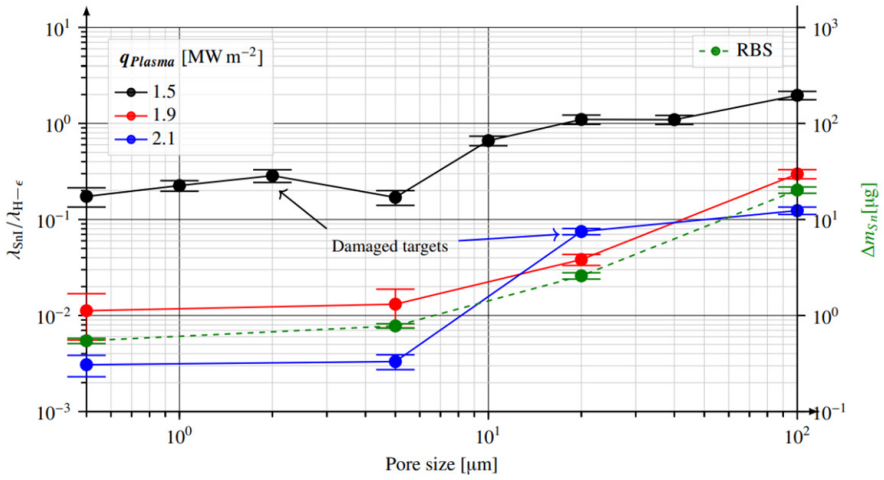

Figure 7 Sn erosion measured on s.s. targets with a different pore size, when exposed to different heat fluxes in Magnum-PSI. The solid lines are the tin emission (326.23 nm) normalized over hydrogen H-ϵ emission line. For the higher heat flux scenarios, the Balmer emission increased faster than the tin emission, hence the lower curve. The error bar in the graph is the covariance of the normalized Gaussian emission line. The dashed green line shows the total tin erosion measured by the RBS on the replaced WPs (i.e., q = 1.9 and q = 2.1 MWm^{-2}). On all targets exposed to q = 1.5 MW m^{-2} no measurable Sn amount could be detected on the WPs using RBS(< 20 ng). Both the Sn emission and the Sn deposition on the WPs decrease a factor 50 when going from 100 µm to 5 µm.

WO_3 core-shell fibers for gas-phase photoelectrochemical water splitting

M. Lavorenti, P. P. Kunturu, and M. N. Tsampas (DIFFER)

In the photoelectrochemical research, many efforts are put into a development of highly efficient materials, which, in many cases, can only be prepared in a very small scale and an industrial fabrication would not be feasible. In case of WO_3 photoabsorber, the material is very accessible and can be prepared on large scale by simply calcinating W samples in air atmosphere. We evaluated performance of gas-phase photoelectrochemical device by functionalization of WO_3@W core-shell fibers in form of a mesh. The functionalization was done by ionomer coating which ensures not only the water absorption but also enhances proton transfer across the electrode-electrolyte interface to enable water splitting into O_2 and H_2. In order to evaluate the ability of the ionomer to deliver enough water for the hydrogen production without any mass transfer limitations, we artificially increased the photocurrent from the WO_3@W photoelectrode by using an LED lamp with 405 nm wavelength matching the absorption spectra of the material. Potentially the photoabsorber can be replaced by mixed oxides such as $BiVO_4$ or perovskites but the need for ionomer functionalization is essential for ambient humidity device operation [Zafeiropoulos, G. et al. ACS Appl. Energy Mater. 4 (2021) 9600, ACS Appl. Mater. Interfaces 11 (2019) 41267] To characterize further our WO_3@W photoelectrodes, we used the ion beam coupled with the RBS detector to analyze the depth of annealing or the thickness of the WO_3 layer. The thickness of the oxide layer determines the light absorption capability but with the increment of it above 150 nm, there is higher probability of electron-hole recombination which decreases the incident photon-to-electron conversion efficiency. Once we used our typical annealing procedure of 6 h the ion beam was not sufficient to reach the W substrate and therefore we decided to anneal our samples for two hours only and then extrapolate the thickness of the layer grown over 6 h. As seen in the Figure 8 bellow, the 6 h samples do not reach the W baseline curve compared to the 2 h samples which start at the WO_3 curve and have a sudden increment in counts which translates to W layer encounter. From the results we could determine the thickness of 2.8 μm for the 2 h calcinated samples and above 6 μm for the 6 h ones.

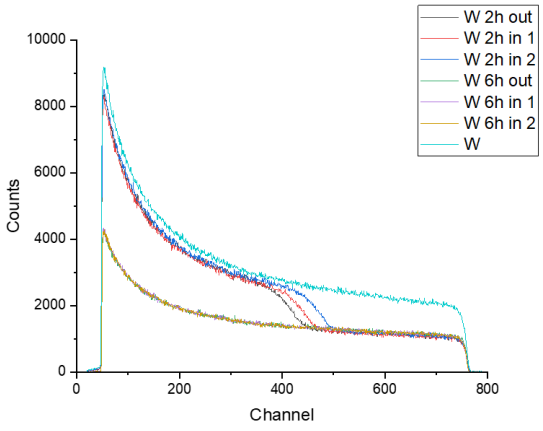

Figure 8 RBS spectra of samples annealed for two and six hours. The latter samples show thick oxide layer where the technique did not reach the W substrate depicted by the turquoise curve

Dynamic deuterium outgassing in tungsten in UPP

Joey Demiane and Maria Morbey (DIFFER)

Dynamic outgassing is the passive desorption of deuterium from a sample within a few hours after exposure. For commercial tokamaks the time during the pulses will have to be shrunk as much as possible. If after each pulse, deuterium is outgassed from the walls time will be required to pump down to acceptable vacuum conditions before the next pulse. Therefore we need to understand the times involved in the outgassing process and what affects retention and subsequent outgassing.

UPP offers the possibility of performing ion beam diagnostics as soon as the plasma exposure is finished. Two parameters were studied, plasma fluence and sample roughness. The fluences varied as follows: 4.3×10^{24} - 4.3×10^{25} - 4.3×10^{26} m^{-2}, the plasma flux was kept constant and the exposure time was increased from 100s to 1000s and 10000s. To increase the sample roughness by means of the Murakami reagent 10wt.% KOH in H^2O and 10 wt.% K3[Fe(CN)6] in H^2O. By changing the time which the sample was immerged in the reagent different roughness were achieved.

NRA was used to determine the deuterium content in each sample. The time after plasma exposure at which NRA was performed was: 30s, 15min, 45 min, 90min, 135min. 180 min and 225 min. When NRA was performed for the sample exposed to 10000s D plasma, a hole in the foil was detected leading to corrupted data, preventing any analysis. Due to the lack of D(3He,p)4He cross-section at the angle of the NRA detector, no qualitative data is available. In the figure below we can see the area under the D peak over time. Roughness increases as follows: W4, W7, W8, W9. However W9 had high C content, therefore it should be disregarded. There is almost no difference between W8 and W4 but W7 shows a sharp decrease between 15min and 45 min, there is no obvious explanation for this observation. For fluence we can only compare W4 and W5, it appears that higher fluence leads to retention decrease which is surprising. Given the results it is clear that further investigation is required, for both roughness and fluence. However these measurements should only be performed once the NRA detector angle in UPP has been modified to an angle where the cross section is known.

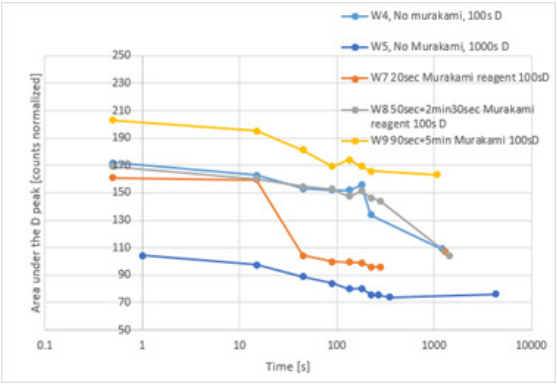

Figure 9 Time evolution of Deuterium outgassing. There is no clear conclusion from the data

Deuterium retention in Li-D co-deposits at higher temperatures and D desorption

Maria Morbey and Thomas Morgan (DIFFER)

In 2021 lithium and deuterium co-deposits were studied with both NRA and EBs. The temperature of the substrate, where the LiD co-deposits formed, was varied by means of a heater in order to study the influence of substrate temperature in retention levels. However, in general, no temperature dependence was observed. This year to achieve a higher T, a new heater was used. Temperatures of 515°C and 450°C were reached and in such temperatures no deuterium retention was detected. Besides higher T of the substrates, desorption after plasma exposure has also been studied. After plasma exposure NRA was performed and subsequently the target holder was moved to the target chamber. There the heater is turned on again for 1 hour. Once the temperature is low enough NRA is once again performed. Moreover, to study the influence of surface morphology only half of the samples were polished. The data has yet to be analyzed. However, some observations can already be done with the raw data, the summary is in the table below.

Table 2 Summary of the observations done with the raw data. P stands for the polished witness plate and R for the rough (non-polished)

	Temp set [°C]	Actually measured Temperature [°C]				Temp set [°C]	Actually measured Temperature [°C]		
		BEFORE PLASMA		DURING PLASMA		DESORPTION	DESORPTION		Comment of Li and D content
	Heater	Temp. polish	Temp rough	Temp. polished	rough	Heater	polished	rough	
ROSC2 Tue+ Wed	OFF	30	?	270	?270	300 (55min)	297	300	There was Li and D on both, after heating there was a decrease in D
ROSC1 Thu	500	430	500	517	?580	-	-	-	There was no D
ROSC3 Friday	300	317	300	448	?460	500 (35min)	540	500	There was D and Li on R but only L on P. All desorbed af-ter the heating. still Li on both
ROSC4 Tue	250	273	250	415 (15:37:17)	413 (15:37:15)	400 (1 hour)	418	400	No D on polished, and little L. A lot of Li and D on rough. All D desorbed from R
ROSC5 Wed	275	265	275	393 (13:38:02)	404 (13:38:02)	-	-	-	-
ROSC5 Wed	275	256	275	414 (14:03:26)	426 (14:03:27)	300 (1 hour + 35min)	284	300	Similar Li and D in P and R. Desorption after 1 hour is clear, no Li lost. Desorption after 1 hour + 35min is clear. No Li lost. We did IB on Thursday morning and it looks the same, no loss of D.

High n Members of Ruddlesden-Popper $La_{n+1}Ni_nO_{3n+1}$ for Oxygen Evolution Reaction

T.P. Le (University of Twente), B. Tyburska-Pueschel, and A. Bieberle (DIFFER)

The electrolysis of water is of great importance to store renewable energy via green hydrogen. However, its efficiency is largely limited by oxygen evolution reaction (OER) activity, where the high overpotential is required to evolve oxygen. Extensive theoretical and experimental work has achieved OER activity enhancement of oxide catalysts based on the material design principles, also called descriptors. The e_g electronic orbital occupancy was found as one such descriptor, where the optimum OER activity was shown for eg orbital filling close to unity (J. Suntivich et.al, Science 303 (2011) 1383) but making high-performance catalysts based on this design principle remains difficult.

Here, we will investigate the OER activity of the high *n* members of Ruddlesden-Popper layered nickelate perovskites, $La_{n+1}Ni_nO_{3n+1}$, by pulsed laser deposition. We will be able to tune the e_g occupancy with *n*, allowing us to tune OER activity. The growth conditions for a stoichiometric $LaNiO_3$ perovskite building block are required to achieve high-quality stoichiometric $La_{n+1}Ni_nO_{3n+1}$ thin films.

Rutherford Backscattering Spectroscopy is used to determine the absolute La:Ni ratio in $LaNiO_3$ thin films as a function of laser fluence. Initial results showed that laser fluence of 1.9 J/cm^2 resulted in the $LaNiO_3$ with La:Ni ratio of 54:46. A further optimization will be carried out.

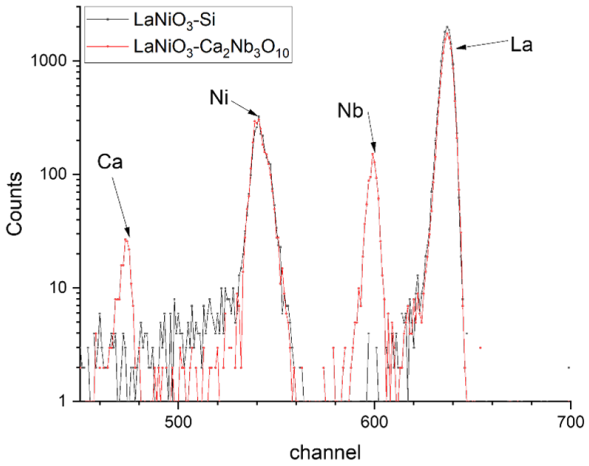

Figure 10 RBS spectra of $LaNiO_3$ films on different substrates

Plasma Exposure of Additively Manufactured Tungsten Coatings

Ben Evans (Oxford University) and Maria Morbey (DIFFER)

Thick tungsten coatings have been produced on steel and tungsten substrates via two additive manufacturing processes as potential alternative processing routes for plasma facing components. Survival of these components under plasma exposure is vital, so testing in fusion-relevant conditions is of paramount importance. Studies on W substrates are for potential in-situ repair applications which could significantly decrease the time taken for repairs. Tungsten coatings have been made using Spark Plasma Sintering (SPS, also known as FAST) on steel and tungsten substrates. There are three strands of research: (A) Erosion/surface (and ELM) damage; (B) thermal cycling; and (C) Deuterium Retention. Deuterium retention was studied by means of ion beam in IBAS. All samples show carbon, however the VPS ones present less carbon. Deuterium retention is only observed in C304. C302 shows no little carbon (only on the edge) and no retention. C303 has carbon,

Reference measurements of outgassing, recycling, and retention after D plasma loading: absolute content and composition in W and reference

Hennie van der Meiden, Beata Tyburska-Pueschel, and Jordy Vernimmen (DIFFER)

For the study of tritium retention in plasma facing components (PFCs) Laser Induced Breakdown Spectroscopy (LIBS) and NRA (giving absolute retained D) are being deployed in Magnum-PSI. A LIBS-based retention monitor will be applied in the JET tokamak in 2024, for measuring D and T retention (after DT operation) but this method still has to be benchmarked against proved techniques such as NRA. Monitoring of T retention is required, because only a certain total amount of T in the ITER vessel is allowed for reasons of radioactivity; moreover the loss of T (a fusion fuel) in the walls needs to be monitored. Various tungsten coating were exposed to pure D plasma and D plasma seeded with 6% helium, nitrogen or neon. The D retention depends on type of seeding and coating (see figure 11), whereas D diffusion depth is influenced only by the type of coating.

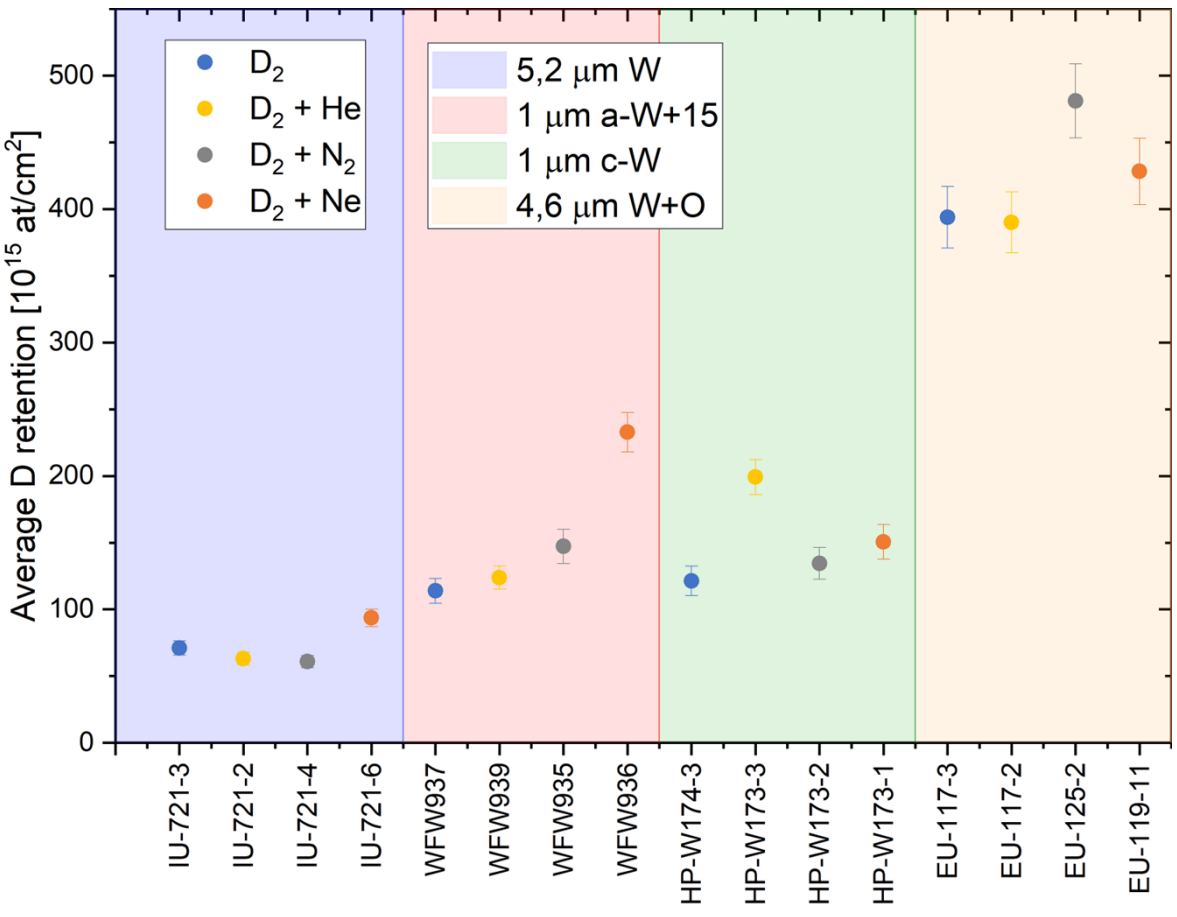

Figure 11 D retention in coatings: 5.2 µm W on Mo (blue), 1 µm amorphous W + 15%O on Mo (red), ~1 µm columnar W on Mo (green), and ~4.6 µm W on Mo (yellow)

Publications

1

F.M. Sapountzi, M. Lavorenti, W. Vrijburg, S. Dimitriadou, B. Tyburska-Pueschel, P. Thüne, H. Niemantsverdriet, T.V. Pfeiffer, M.N. Tsampas, Spark Ablation for the Fabrication of PEM Water Electrolysis Catalyst-Coated Membranes, Catalysts 12 (2022) 1343; https://doi.org/10.3390/catal12111343

2

D. Chaykina, I. Usman, G. Colombi, H. Schreuders, B. Tyburska-Pueschel, Z. Wu, S.W.H. Eijt, L.J. Bannenberg, G.A. de Wijs, B. Dam, Aliovalent Calcium Doping of Yttrium Oxyhydride Thin Films and Implications for Photochromism, J. Phys. Chem. C 126 (2022) 14742−14749; https://doi.org/10.1021/acs.jpcc.2c04456

3

J.G.A. Scholte, M. Iafrati, S.S.H. Lam, B. Tyburska-Pueschel, M. Riepen, F. Brochard, M.M.P. Vissers, T.W. Morgan, Reducing tin droplet ejection from capillary porous structures under hydrogen plasma exposure in Magnum-PSI, Nuclear Materials and Energy (2022); https://doi.org/10.1016/j.nme.2022.101315

DIFFER

Dutch Institute for Fundamental Energy Research
De Zaale 20
5612 AJ Eindhoven

PO Box 6336
NL-5600 HH Eindhoven
The Netherlands

info@differ.nl
www.differ.nl

DIFFER

SCIENCE FOR **FUTURE ENERGY**